

**Figure S1. Characterization of LAKI 4F TTFs upon Short-Term Induction of OSKM, Related to Figure 1**

(A) qPCR analysis of *Oct4*, *Sox2*, *Klf4* and *c-Myc* in LAKI 4F tail tip fibroblasts (TTFs). \*\* $p < 0.005$ , \*\*\* $p < 0.0005$  and \*\*\*\* $p < 0.0001$ , according to one-way ANOVA with Bonferroni correction.

(B) Analysis of cellular identity of LAKI 4F TTFs following partial reprogramming analyzed by flow cytometry using Thy1 and SSEA1 staining.

(C) qPCR analysis of *Nanog* expression in LAKI 4F TTFs after short-term induction of OSKM by doxycycline treatment.

(D) Quantification of foci intensity and foci volume of  $\gamma$ H2AX staining in LAKI 4F TTFs. \*\*\*\* $p < 0.0001$ , according to one-way ANOVA with Bonferroni correction.

(E) Immunostaining of 53BP1 in LAKI 4F TTFs following doxycycline treatment. The number, volume, and intensity of 53BP1 foci in LAKI 4F TTFs were quantified in Oct4 positive and negative cells. Scale bar, 10  $\mu$ m. \* $p < 0.05$ , \*\* $p < 0.01$ , \*\*\* $p < 0.0005$  and \*\*\*\* $p < 0.0001$ , according to one-way ANOVA with Bonferroni correction.

(F)  $\beta$ -galactosidase activity in WT and LAKI 4F TTFs. Quantification of cells with  $\beta$ -galactosidase staining. Scale bar, 100  $\mu$ m. \*\*\* $p = 0.001$  and \*\*\*\* $p < 0.0001$ , according to one-way ANOVA with Bonferroni correction.

(G) Levels of mitochondrial ROS in LAKI 4F TTFs after doxycycline treatment. \*\* $p < 0.01$ , according to one-way ANOVA with Bonferroni correction.

Data are presented as mean  $\pm$  SEM.

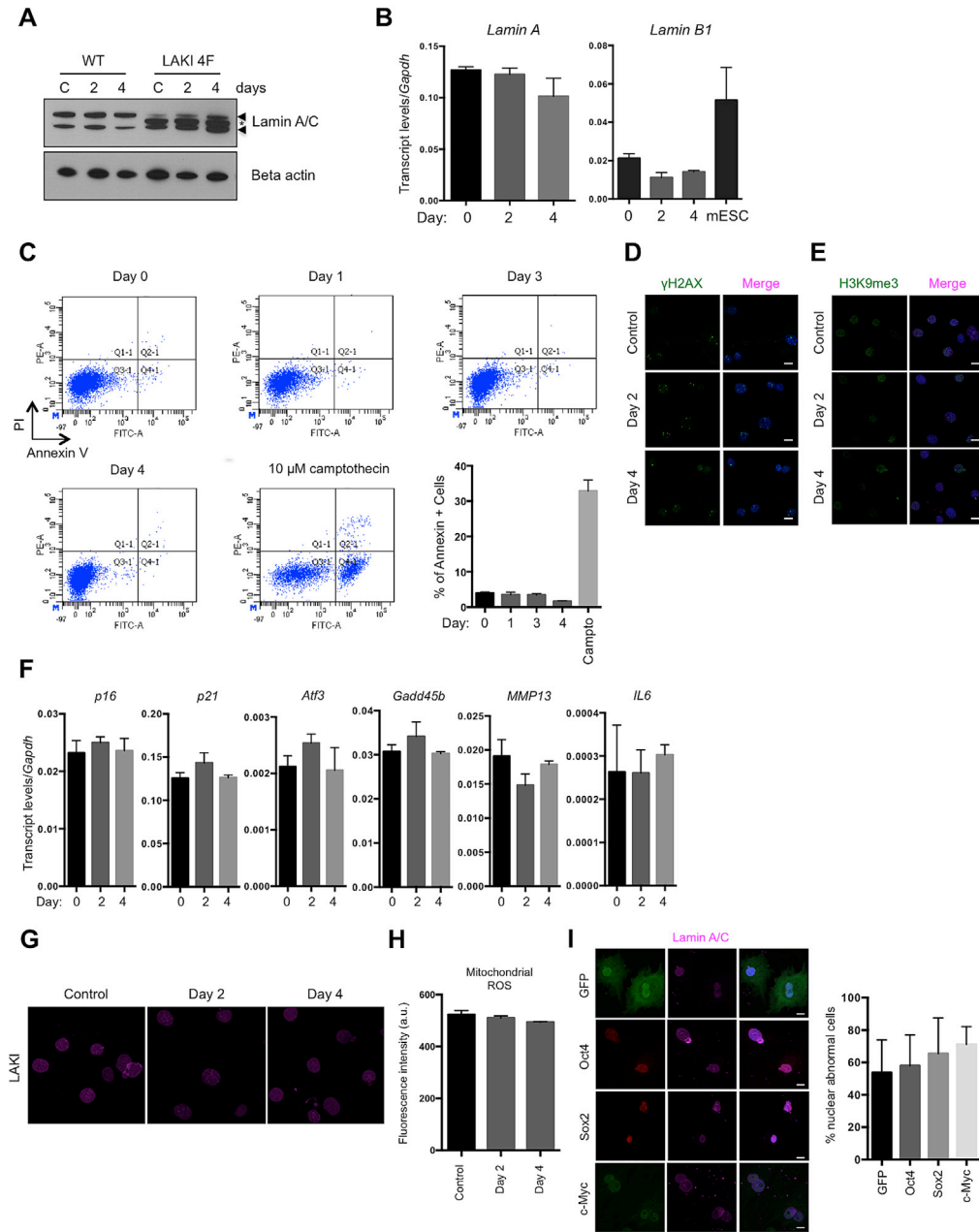


**Figure S2. Characterization of LAKI 4F and LAKI TTFs following Doxycycline Treatment, Related to Figure 1**

(A) Detection of Lamin A/C and progerin levels in WT 4F and LAKI 4F TTFs after short-term doxycycline treatment by western blot. Arrowheads denote Lamin A and C. Asterisk denotes progerin.

(B) qPCR analysis of *Lamin A* and *Lamin B1* levels in LAKI 4F TTFs.

(C) Analysis by flow cytometry of programmed cell death in LAKI 4F TTFs following doxycycline treatment.

(D) Immunofluorescence of  $\gamma$ H2AX in LAKI TTFs following doxycycline treatment.

(E) Immunofluorescence of H3K9me3 in LAKI TTFs following doxycycline treatment.

(F) qPCR analysis of stress response genes in the p53 pathway, senescence-associated metalloprotease *MMP13* and *interleukin-6* in LAKI TTFs following doxycycline treatment.

(G) Immunofluorescence of Lamin A/C in LAKI TTFs following doxycycline treatment.

(H) Levels of mitochondrial ROS in LAKI TTFs after doxycycline treatment.

(I) Immunofluorescence of Oct4, Sox2, c-Myc and Lamin A/C in LAKI TTFs infected with GFP, Oct4, Sox2 and c-Myc retroviruses. Scale bar, 10  $\mu$ m.

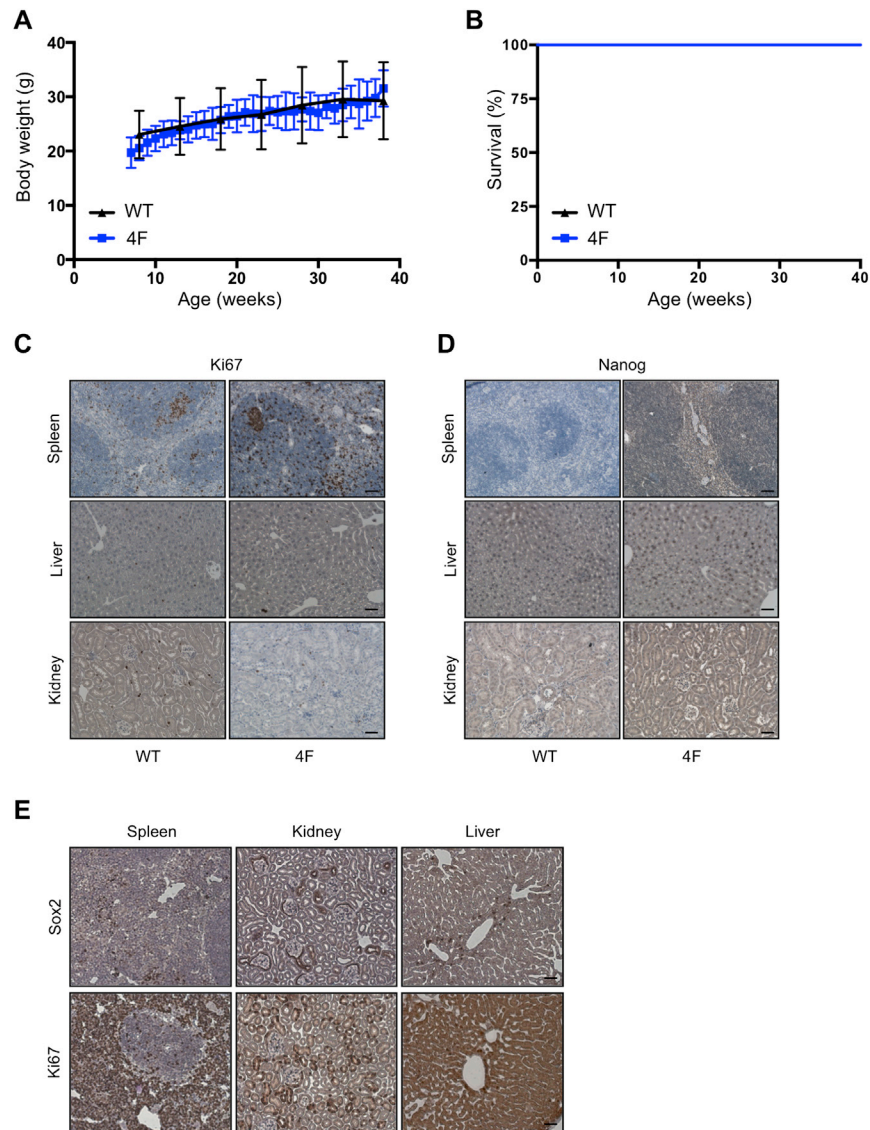


**Figure S3. Effect of Long-Term In Vivo Cyclic Induction of *Oct4*, *Sox2*, *Klf4*, and *c-Myc* in Mice Carrying One and Two Copies of OSKM and rtTA Cassette, Related to Figure 3**

(A) Body weight of wild-type (WT) and 4F mice carrying single copy of OSKM and rtTA cassette upon cyclic administration of doxycycline. WT (n = 5) and 4F (n = 3).

(B) Survival of WT and 4F mice carrying single copy of OSKM and rtTA cassette upon cyclic administration of doxycycline. WT (n = 5) and 4F (n = 3).

(C and D) Immunostaining of Ki67 and Nanog in spleen, liver, and kidney of WT and 4F mice carrying single copy of OSKM and rtTA cassette. Scale bar, 100  $\mu$ m (spleen) and 50  $\mu$ m (liver and kidney).

(E) Immunostaining of Sox2 and Ki67 in spleen, liver, and kidney of 4F mice carrying two copies of OSKM and rtTA cassette. Scale bar, 50  $\mu$ m.

Data are presented as mean  $\pm$  SEM.

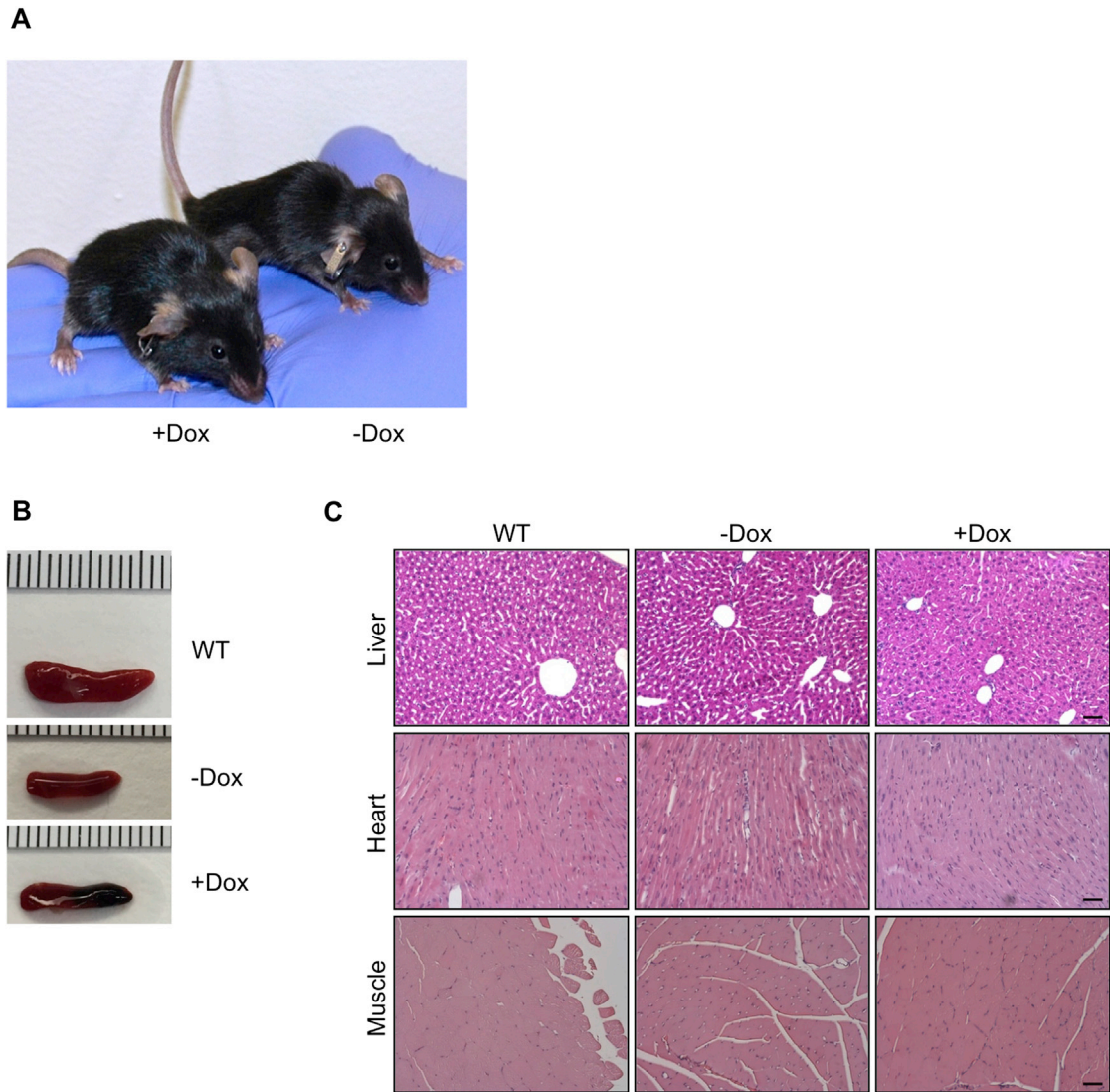


**Figure S4. Characterization of LAKI 4F Mice Subjected to Cyclic Induction of OSKM, Related to Figure 4**

(A) Representative picture of LAKI 4F mice at 16-weeks of age upon doxycycline administration. Curvature of spine can be observed in LAKI 4F not treated with doxycycline (-Dox).

(B) Partial rescue of spleen involution is observed in LAKI 4F mice upon doxycycline administration.

(C) Histological analysis of liver, heart, and muscle of WT and LAKI 4F mice upon cyclic doxycycline administration. Scale bar, 50  $\mu$ m.

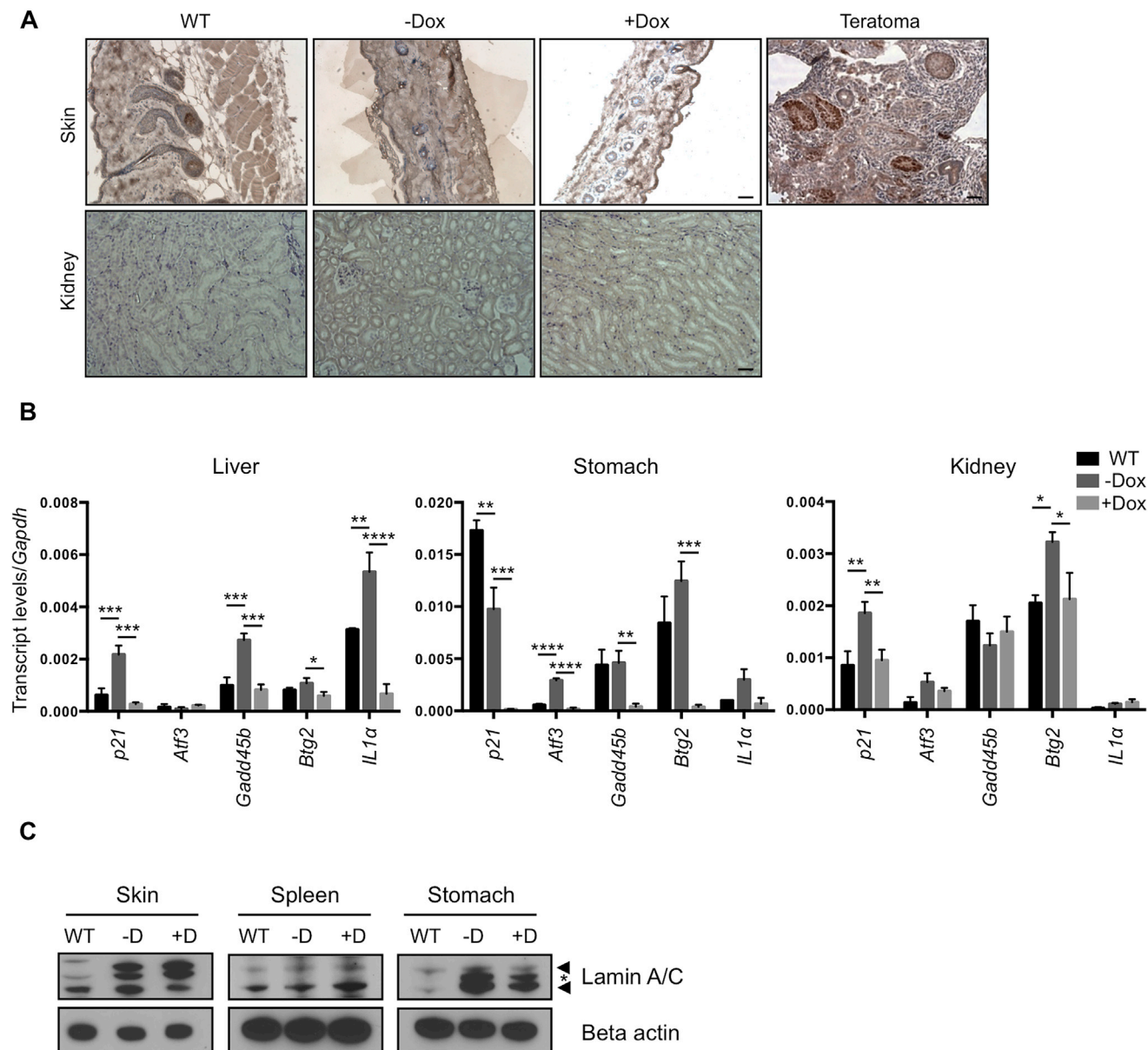


**Figure S5. Molecular Changes Induced by Cyclic In Vivo Induction of *Oct4*, *Sox2*, *Klf4*, and *c-Myc*, Related to Figure 5**

(A) Immunohistochemistry of Nanog in skin and kidney of WT and LAKI 4F mice upon cyclic doxycycline administration. Teratoma was used as a positive control. Scale bar, 50  $\mu$ m.

(B) qPCR analysis of stress response genes in the p53 pathway and *interleukin-1 $\alpha$*  in liver, stomach, and kidney of LAKI 4F mice upon cyclic doxycycline administration. \* $p < 0.05$ , \*\* $p < 0.01$ , \*\*\* $p < 0.0001$  and \*\*\*\* $p < 0.0001$ , according to one-way ANOVA with Bonferroni correction.

(C) Detection of Lamin A/C and progerin levels in skin, spleen, and stomach of WT and LAKI 4F mice by western blot. Arrowheads denote Lamin A and C. Asterisk denotes progerin.

Data are presented as mean  $\pm$  SEM.

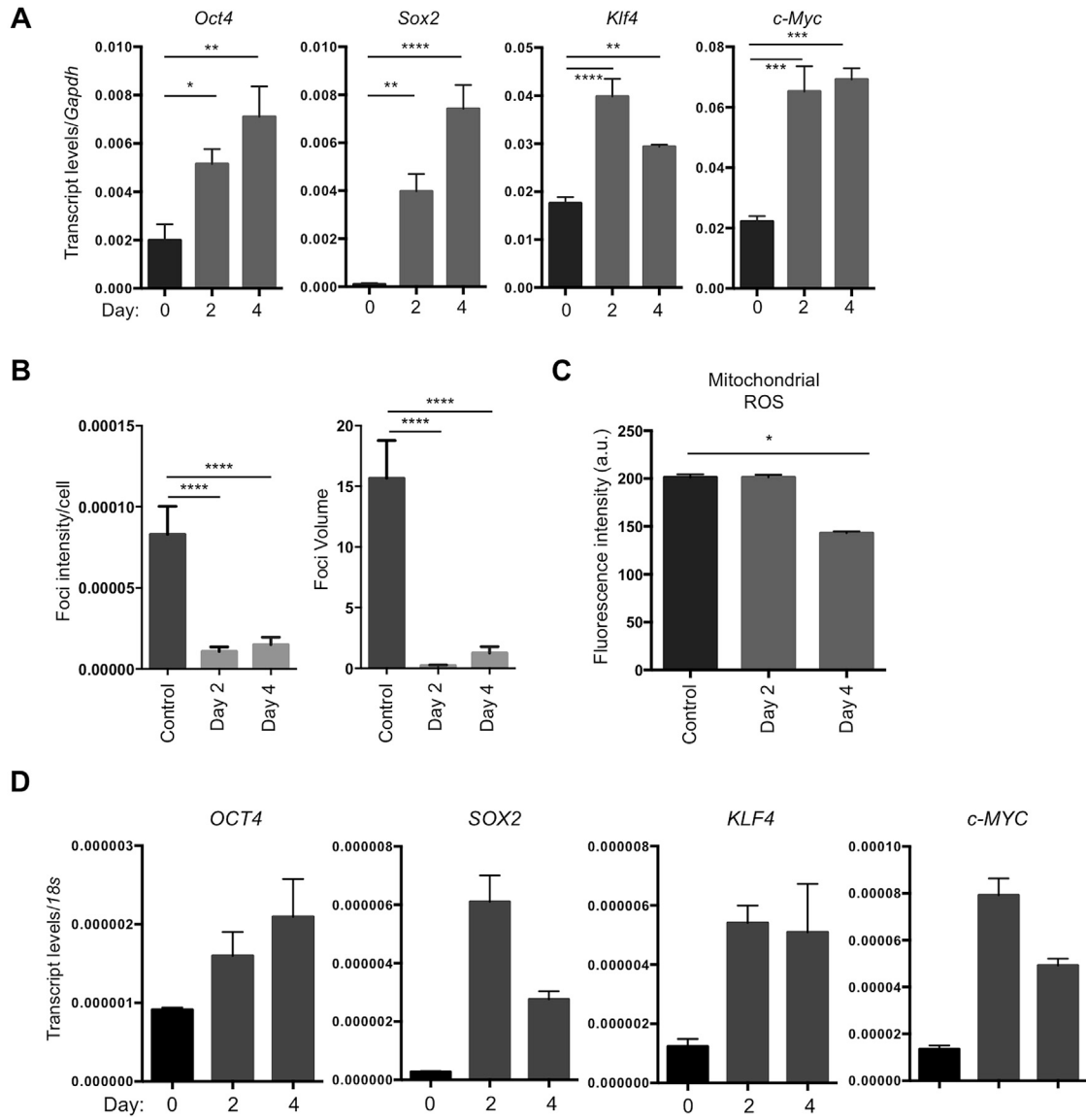


**Figure S6. Amelioration of Aging-Associated Phenotypes in Wild-Type Mice and Human Cells by Short-Term Expression of Reprogramming Factors, Related to Figure 6**

(A) qPCR analysis of *Oct4*, *Sox2*, *Klf4* and *c-Myc* in WT 4F TTFs. \* $p < 0.05$ , \*\* $p < 0.05$ , \*\*\* $p < 0.005$ , \*\*\*\* $p < 0.0001$ .

(B) Quantification of foci intensity and foci volume of  $\gamma$ H2AX staining in WT 4F TTFs. \*\*\*\* $p < 0.0001$ , according to one-way ANOVA with Bonferroni correction.

(C) Analysis of ROS levels in LAKI 4F TTFs after doxycycline treatment. \* $p < 0.05$ , according to one-way ANOVA with Bonferroni correction.

(D) qPCR analysis of *OCT4*, *SOX2*, *KLF4* and *c-MYC* in human 4F fibroblasts.

Data are presented as mean  $\pm$  SEM.

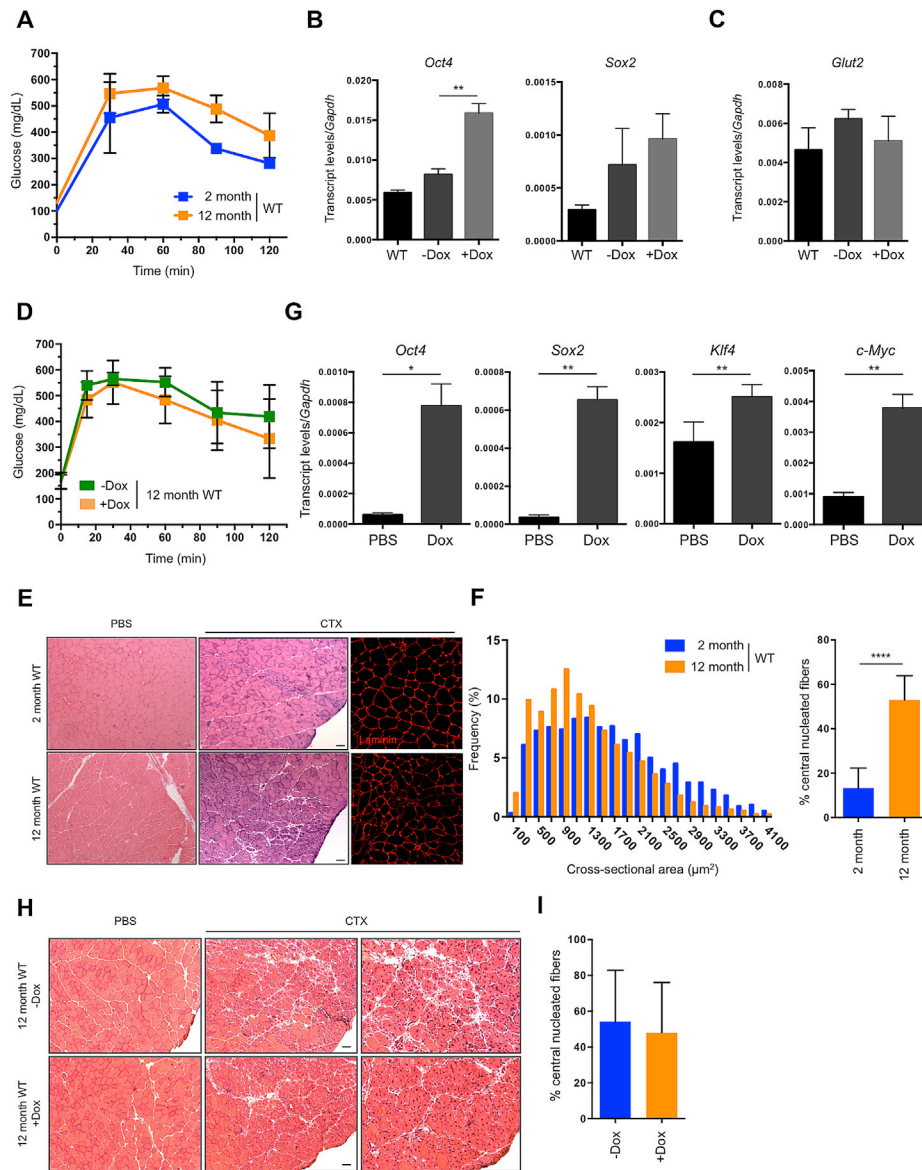


**Figure S7. Analysis of Pancreatic Function and Skeletal Muscle Regeneration in Wild-Type Mice, Related to Figure 7**

(A) Glucose tolerance test (GTT) in 2-month and 12-month old WT mice following beta cell ablation by low dose (50 mg/kg) STZ (2-month WT n = 3; 12-month WT n = 3).

(B) qPCR analysis of *Oct4*, *Sox2*, in pancreas of 12-month old WT 4F mice upon administration of doxycycline. \*\*p < 0.01, according to one-way ANOVA with Bonferroni correction.

(C) qPCR analysis of *Glut2* in pancreas of 12-month old WT 4F mice upon administration of doxycycline.

(D) GTT in 12-month old WT mice following doxycycline and beta cell ablation by low dose (50 mg/kg) STZ (-Dox n = 5; +Dox n = 5).

(E) Representative image of H&E staining and immunostaining of Laminin of tibialis anterior (TA) muscle of 2-month and 12-month old WT mice following muscle injury by CTX injection. Scale bar, 50 μm.

(F) Quantification of fiber cross-sectional area frequency distribution and percentage of central nucleated fibers in muscle sections of 2-month and 12-month old WT mice following muscle injury by CTX injection. (2-month WT n = 3; 12-month WT n = 3). \*\*\*\*p < 0.0001, according to two-tailed Student's t test.

(G) qPCR analysis of *Oct4*, *Sox2*, *Klf4* and *c-Myc* in skeletal muscle of 12-month WT 4F mice upon administration of doxycycline. \*p < 0.05, \*\*p < 0.01, according to two-tailed Student's t test.

(H) Representative low- and high-magnification images of H&E staining of TA muscle of 12-month-old WT mice following doxycycline treatment and muscle injury by CTX injection. Scale bar, 50 μm.

(I) Quantification of percentage of central nucleated fibers in muscle sections of 12-month old WT mice following doxycycline treatment and muscle injury by CTX injection (-Dox n = 3; +Dox n = 3).